

[3]. The values found for the coefficients A_k , B_k , D_k , and E_k were used to calculate the velocity distribution and the resistance coefficient of the rotating channel. Figure 1 shows the calculated values of the resistance coefficient of the channel λ_ω/λ_0 as a function of the parameter $\sqrt{R/2}$ for various values of l/h . For fixed R the resistance coefficient of the channel increases with an increase in its extension in a direction perpendicular to the axis of rotation. For fixed l/h and small values of R the ratio λ_ω/λ_0 is proportional to R ; for $R > 300$ the dependence of λ_ω/λ_0 on $\sqrt{R/2}$ is practically linear. This shows that for large R the main contribution to the channel resistance comes from the Ekman layer formed on the channel walls perpendicular to the axis of rotation.

The lack of experimental data prevents a direct comparison of our calculated results with experiment. A comparison of the theoretical values of the resistance coefficient with the corresponding values of λ_ω obtained by extrapolating the experimental law $\lambda_\omega = \lambda_\omega(R_0)$ for $R = \text{const}$ in the range of small Rossby numbers shows good agreement for a channel with a square cross section for all values of R .

LITERATURE CITED

1. H. Greenspan, *The Theory of Rotating Fluids*, Cambridge Univ. Press (1969).
2. O. N. Ovchinnikov and E. M. Smirnov, "Flow dynamics and heat transfer in a rotating slot channel," *Inzh.-Fiz. Zh.*, 35, No. 1 (1978).
3. S. B. Nikol'skaya, "Laminar motion of a fluid in rotating channels," *Izv. Akad. Nauk SSSR, Mekh. Zhidk. Gaza*, No. 6 (1977).

MOTION OF A PLANE PLATE OF FINITE WIDTH IN A VISCOUS CONDUCTIVE LIQUID, PRODUCED BY ELECTROMAGNETIC FORCES

V. I. Khonichev and V. I. Yakovlev

UDC 538.4

Studies are available [1-4] which demonstrate the possibility, in principle, of creating magnetohydrodynamic engines for marine vessels. They have demonstrated that due to the low conductivity of seawater and the limited value of the magnetic fields employed, the efficiency of such engines will be low. However, recent successes in development of superconductive materials permit the hope of increased field intensities in such magnetic systems, and consequently, increased efficiencies in such MHD engines. It is thus of interest to study the peculiarities of flow around bodies in the vicinity of which volume electromagnetic forces produced by a source within the body flowed over exist.

1. The present study is dedicated to examination of the motion of the simplest model of a body (a plate of finite width) in a viscous conductive liquid. Numerical solution of the Navier-Stokes equation together with the equation of motion of the solid will determine the velocity of the plate's translational motion relative to the liquid which is at rest at infinity, and also the pattern of flow around the plate; the plate is set in motion by a magnetic field in the form of a traveling wave created by surface currents distributed over the plate width. The presence of turbulent volume forces in the liquid near the plate set in motion in this electromagnetic fashion makes the flow pattern different from the classical one.

Because of the numerical method used to solve the Navier-Stokes equation the flow under study must be limited to Reynolds number values on the order of magnitude of 10^3 .

Thus, we will consider a plane plate of width $2a$ along the x axis, infinite in extent along the z axis, and located in an infinite viscous conductive liquid. Along the z axis a surface current

$$i_z(x_1, t) = i_0(x_1) e^{i(k_1 x_1 - \omega t)} (|x_1| \leq a) \quad (1.1)$$

flows over the plate in the form of a traveling wave with amplitude varying with x . We will consider the case $i_0(x_1) = I_0 \cos(\pi x_1/2a)$. It is necessary to find the electric and magnetic field distributions, the distribution of volume forces $\mathbf{f} = (1/c)[\mathbf{j} \times \mathbf{H}]$ in the conductive liquid, and the force acting on the plate carrying the current of Eq. (1.1) due to the magnetic field of the currents induced in the liquid. On this basis we must determine the velocity v_0 taken on by the plate, and the field of liquid flow velocities relative to the plate.

2. The electric and magnetic fields will be determined on the assumption that the effect of liquid flow on electromagnetic processes may be neglected. This will be valid given a sufficiently small magnetic Reynolds number

$$\text{Re}_m = 4\pi\sigma v_0 2a/c^2 \ll 1. \quad (2.1)$$

Since the number Re_m is related to the hydrodynamic Reynolds number Re by the expression $\text{Re}_m = (v/v_m)\text{Re}$, where $v, v_m = c^2/4\pi\sigma$ are the kinematic and magnetic viscosities, for seawater with $\sigma = 5 \cdot 10^{10}/\text{lc}_1$, $v = 10^{-2} \text{ cm}^2/\text{sec}$ we have $v/v_m \approx 10^{-11}$, i.e., $\text{Re}_m \approx 10^{-11}\text{Re}$. Consequently in the range considered here $\text{Re} \sim 10^3$ condition (2.1) is satisfied to a high degree of accuracy.

Given condition (2.1), the vector potential $A_1(x_1, y_1, t) = A_1(x_1, y_1) e^{-i\omega t} \mathbf{e}_z$ describing the electromagnetic field is determined by the following dimensionless equations and boundary conditions:

$$\Delta A(x, y) + (2i/\delta^2) A(x, y) = 0; \quad (2.2)$$

$$\left. \frac{\partial A}{\partial y} \right|_{y=0} = \begin{cases} -\cos \pi x \cdot e^{ik_0 x} & \text{for } |x| \leq 1/2, \\ 0 & \text{for } |x| > 1/2; \end{cases} \quad (2.3)$$

$$A|_{y=\infty} = 0. \quad (2.4)$$

The physical system under consideration is symmetric relative to the plane $y = 0$, so we take the semiplane $y > 0$ as the region for definition of the function $A(x, y)$. The dimensionless quantities in Eqs. (2.2)-(2.4) have the form

$$x = x_1/2a, y = y_1/2a, A = A_1/2aH_0, H_0 = 2\pi I_0/c_x \quad (2.5)$$

i.e., for the scale factors for length, magnetic field intensity, and vector potential we take $2a, H_0, 2aH_0$, while the dimensionless depth of the skin-layer δ and the wave number k_0 will equal

$$\delta = \frac{1}{2a} \frac{c}{\sqrt{2\pi\sigma\omega}}, \quad k_0 = k_1 2a. \quad (2.6)$$

The wave number k_0 determines the number n of half-waves of current included over the plate width. In fact, $k_0 = (2\pi/\lambda)2a = n\pi$, where $n = 2a/\lambda/2$. Using a Fourier transformation in the variable x , we reduce the solution of Eqs. (2.2)-(2.4) to the form

$$A(x, y) = - \int_{-\infty}^{\infty} J(k) \frac{e^{-\sqrt{k^2 - 2i/\delta^2} y}}{\sqrt{k^2 - 2i/\delta^2}} e^{ikx} dk, \quad J(k) = \frac{\cos \frac{k - k_0}{2}}{(k - k_0)^2 - \pi^2}, \quad (2.7)$$

where by $\sqrt{k^2 - 2i/\delta^2}$ we understand a complex value with positive real component, i.e.,

$$\sqrt{k^2 - 2i/\delta^2} = r(k) - is(k), \quad r(k) > 0. \quad (2.8)$$

3. We will use solution (2.7) to calculate the volume force rotor $\mathbf{f} = (1/c) \mathbf{j} \times \mathbf{H} = (\sigma/c) [\mathbf{E} \times \mathbf{H}]$ and the forces acting on the plate.

It is known (see, e.g., [5]) that in a varying electromagnetic field the volume forces have both stationary and oscillating (at a frequency 2ω) components. The same is true of the net force F_x acting on the plate. In the present study we will consider the steady-state motion arising due to the action of the stationary force components, so we will present below expressions only for those components. Since

$$\langle \mathbf{f} \rangle = (\sigma/2c) \text{Real} (EH_x^* e_y - EH_y^* e_x),$$

where

$$E = i(\omega/c) A_1; H_x = \frac{\partial A_1}{\partial y_1}; H_y = -\frac{\partial A_1}{\partial x_1},$$

the desired quantity is equal to

$$\text{rot}_z \langle \mathbf{f} \rangle = (\sigma\omega/2c^2)(I_0/c)^2 \text{Rot} f, \\ \text{Rot} f = 8\pi^2 \text{Real} \left\{ \int_{-\infty}^{\infty} k J(k) e^{-r(k)y} \frac{e^{i[s(k)y+kx]}}{r(k) - is(k)} dk - \int_{-\infty}^{\infty} J(k) e^{-r(k)y} e^{i[s(k)y+kx]} dk \right\}. \quad (3.1)$$

Here, by $\text{Rot} f$ we denote the dimensionless rotor of the volume forces.

We will calculate the projection on the x axis of the net force F acting on the plate due to the magnetic field of currents in the conductive liquid (for a unit plate length along the z axis).

The time-averaged (over the period $2\pi/\omega$) value is defined in the form

$$\langle F_x \rangle = -(1/c) \int_{-a}^a \langle i_z(x_1, t) H_y(x_1, 0, t) \rangle dx_1.$$

Substituting Eq. (2.7) we obtain

$$\langle F_x \rangle = -a(I_0/c)^2 F_1, \quad F_1 = 4\pi^2 \int_{-\infty}^{\infty} \frac{ks(k)}{r^2(k) + s^2(k)} |J(k)|^2 dk, \quad (3.2)$$

where $r(k)$, $s(k)$ are defined by Eq. (2.8). Results of the calculations are presented in Fig. 1, where the dimensionless force F_1 is shown as a function of k_0 for various values of δ .

4. Under the action of the applied force $\langle F_x \rangle$ the plate takes on a translational velocity in the negative x direction. Neglecting the effect of the variable component of the volume forces in the liquid upon the stationary component of the flow (which is valid for $\delta^2 \text{Re}_m \ll 1$), we will study the settled motion of the plate relative to the liquid, which is at rest at infinity. The actual study is conducted in a coordinate system fixed to the plate; we consider the pattern of flow around the plate of a liquid which has a translational velocity v_0 directed along the x axis at infinity.

The defining equations are the hydrodynamics equations with volume forces

$$(\mathbf{v}\nabla) \Omega = \text{Rot} f e_z + (1/\text{Re}^*) \Delta \Omega, \quad (4.1) \\ \mathbf{v} = \frac{\partial \Psi}{\partial y} e_x - \frac{\partial \Psi}{\partial x} e_y, \quad \Delta \Psi = -\Omega,$$

and the equation of motion of the plate, which in the case of steady-state motion reduces to $\langle F_x \rangle + T_x = 0$, where T_x is the resistive force acting upon the plate due to viscosity. In dimensionless form this equation appears as

$$-F_1 + (1/\pi\delta^2)(1/\text{Re}^*) T = 0, \quad T = - \int_{-1/2}^{1/2} \Omega(x, 0) dx. \quad (4.2)$$

The dimensionless velocity v , turbulence Ω , and flow function Ψ in Eqs. (4.1), (4.2) are introduced by means of the scale factors

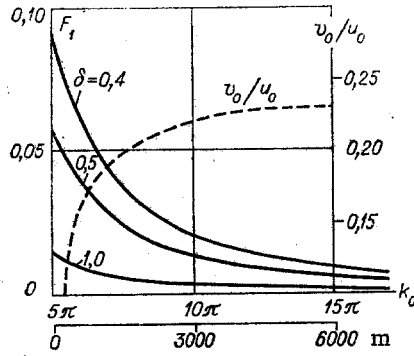


Fig. 1

$$u_0 = (I_0/c)(\delta\sqrt{4\pi\rho})^{-1}, \quad \Omega_0 = u_0/2a, \quad \Psi_0 = 2au_0 \quad (4.3)$$

(where ρ is the liquid density).

It should be noted that the scale velocity used here u_0 (Eq. (4.3)) does not coincide with the velocity of plate motion v_0 . The Reynolds number appearing in Eqs. (4.1), (4.2) is defined by the velocity u_0 and will be denoted by Re^*

$$Re^* = u_0 2a/\nu. \quad (4.4)$$

This value differs from the "true" Reynolds number, defined by the plate motion velocity,

$$Re = v_0 2a/\nu = (v_0/u_0) Re^*. \quad (4.5)$$

The ratio v_0/u_0 is determined during the solution process. Writing the desired function in the form of a sum

$$\Psi(x, y) = (v_0/u_0)y + \psi(x, y), \quad (4.6)$$

we obtain the final equations in the form

$$\left(\frac{v_0}{u_0} + \frac{\partial\psi}{\partial y}\right) \frac{\partial\Omega}{\partial x} - \frac{\partial\psi}{\partial x} \frac{\partial\Omega}{\partial y} - \frac{1}{Re^*} \Delta\Omega = \text{Rot } f; \quad (4.7)$$

$$\Delta\psi = -\Omega; \quad (4.8)$$

$$F_1 + (1/\pi\delta^2 Re^*) \int_{-1/2}^{1/2} \Omega_0(x) dx = 0, \quad \Omega_0(x) = \Omega(x, y)|_{y=0}. \quad (4.9)$$

On the boundary $y = 0$ the boundary conditions for Eqs. (4.7), (4.8) have the form

$$\psi = 0 \quad (-\infty < x < \infty), \quad \Omega = \begin{cases} 0 & \text{at } |x| > 1/2, \\ \Omega_0(x) & \text{at } |x| \leq 1/2 \end{cases} \quad (4.10)$$

at infinity

$$\Omega \rightarrow 0, \quad \partial\psi/\partial y \rightarrow 0.$$

The function $\Omega_0(x)$ appearing in Eqs. (4.9), (4.10) is unknown, and will be determined in the solution process by the adhesion condition, as a consequence of which, on the plate surface, according to Eq. (4.6), the condition

$$\partial\psi/\partial y|_{y=0} = -v_0/u_0 \quad (|x| \leq 1/2)$$

must be satisfied. The right-hand side of Eq. (4.7) is defined in Eq. (3.1).

The numerical solution of the problem was constructed on the basis of Dzhakupov's finite-difference method [6] with a few changes required by the presence of the additional Eq. (4.9) and the additional unknown v_0/u_0 .

The calculation region used was the rectangle formed by the straight lines $y = 0$, $y = 0.295$, $x = -0.7375$, $x = 1.2375$. The grid used spatial steps $\delta x = 0.025$, $\delta y = 0.005$, so that the total number of cells comprised 4661; the δy step chosen was smaller due to the presence of large gradients in the unknowns along the y axis.

In difference format the boundary conditions at $y = 0$ appear as follows:

$$\psi_{i,0} = 0,$$

$$\Omega_{i,0} = \begin{cases} 0 & \text{at } |x| > 1/2, \\ -\frac{8\psi_{i,1} - \psi_{i,2}}{2\delta y^2} - \frac{3v_0}{u_0} \frac{1}{\delta} & \text{at } |x| \leq 1/2 \end{cases}$$

(for a discussion of the latter equation for turbulence, see [7]). On the left ($x = -0.7375$), upper ($y = 0.295$), and right ($x = 1.2375$) boundaries the following relationships are used:

$$\Omega_{0,j} = 0, \psi_{0,j} = \psi_{1,j}, \Omega_{i,N} = 0, \psi_{i,N} = \psi_{i,N-1},$$

$$\Omega_{I,j} = \Omega_{I-1,j} - \Omega_{I-2,j}, \psi_{I,j} = 2\psi_{I-1,j} - \psi_{I-2,j},$$

while with the δx , δy values and size of the calculation region employed $N = 59$, $I = 79$. The difference approximation of Eq. (4.2) has the form

$$\left(\frac{v_0}{u_0}\right)^{(m+1)} = \frac{1}{3} \pi \delta^2 \text{Re}^* F_1 \delta y - \frac{1}{6} \frac{\delta x}{\delta y} \sum_{i=I_1}^{I_2} [8\psi_{i,1}^{(m+1)} - \psi_{i,2}^{(m+1)}],$$

where I_1 , I_2 are the initial and final points of the difference grid on the plate, m is the number of iterations. The algorithm was optimized with a model problem [8].

5. The concrete flow calculation was performed for an electromagnetic field with parameters $k_0 = 14.2\pi$, $\delta = 0.4$, for which the dimensionless force F_1 is equal to 0.0100, while the volume force rotor has the distribution shown in Fig. 2 (Rot f isolines are shown with corresponding values). It is evident that the electromagnetic turbulence sources decay rapidly with removal from the plate; this fact was considered in choosing the calculation region with boundaries passing quite close to the plate. The errors produced by replacing conditions at infinity with boundary conditions on the boundaries of the finite calculation region were studied by varying the size of the calculation region, after which the region used herein was selected. Moreover, for a Reynolds number $\text{Re} = 230.94$ a calculation was performed for flow around the plate without electromagnetic fields (which for the sake of brevity we will term the classical plate), and the plate resistance coefficient c_f thus obtained was compared with the known coefficient [9]

$$c_f^0 = 1.328/\sqrt{\text{Re}} + 4.12/\text{Re}, \quad (5.1)$$

which has been confirmed experimentally [10]. It developed that the difference between the two values was less than 4%: $c_f = 0.1014$, $c_f^0 = 0.1052$. This fact indicates that the inaccuracy in calculation of flow parameters and the leading and trailing edges of the plate which appear because of use of a system with fixed grid also have no noticeable effect on the flow as a whole.

The plate velocity and flow pattern were calculated for Reynolds numbers $\text{Re}^* = 10^3$ and $3 \cdot 10^3$. These correspond (according to the calculation results) to actual values $\text{Re} = 230.94$ and $\text{Re} = 1180.60$. (The numbers Re , Re^* are defined in Eqs. (4.4) and (4.5).)

The calculation results are presented in the form of graphs. The dashed curve in Fig. 1 illustrates the process of approach of the quantity v_0/u_0 to its exact value as the number of iterations m is increased. The maximum number of iterations was 6000; all the examples described here were calculated with that number of iterations. The quantity v_0/u_0 is then equal to 0.23094 at $\text{Re}^* = 10^3$ and 0.39353 at $\text{Re}^* = 3 \cdot 10^3$, whence, according to Eq. (4.5), $\text{Re} = 230.94$ and 1180.60, respectively.

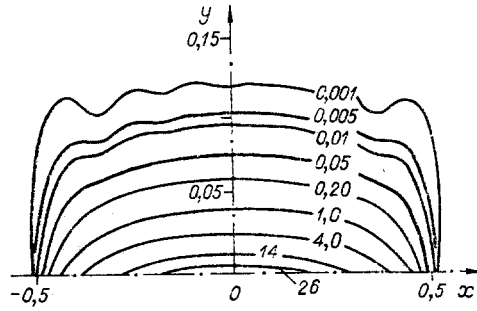


Fig. 2

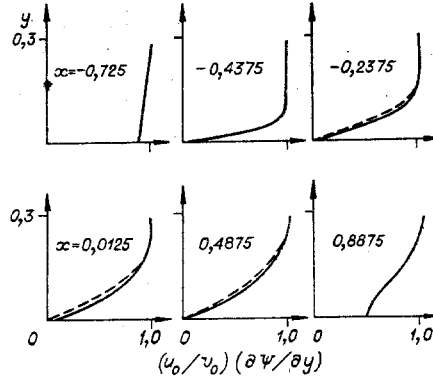


Fig. 3

The calculations revealed that the flow patterns for the classical plate and the plate set in motion by electromagnetic forces coincide qualitatively. This is due to the smallness of the magnetohydrodynamic interaction parameter in plate motion with $Re \sim 10^3$. A concise presentation of the velocity fields can be found in Fig. 3, which shows velocity profiles across the plate in sections $x = \text{const}$ for $Re = 230.94$ (solid lines for presence of electromagnetic field, dashed lines for classical plate). There is a difference in the value of the velocity gradient near the plate; the gradient is larger in the case of the plate with electromagnetic field than in the classical case. This can be seen from Figs. 4, 5, which show isolines of the turbulence $\Omega = \text{const}$ for $Re = 230.94$ for the plate with electromagnetic field (Fig. 4) and the classical plate (Fig. 5). It is obvious that the difference in the Ω distribution for these two cases occurs in the immediate vicinity of the plate and is produced by the effect of the volume force rotor in this region. It is then understandable that the resistance coefficient c_e of the plate with electromagnetic field is higher than the resistance coefficient c_f^0 of the classical plate. We will compare these values for $Re = 230.94$; c_e is found from the relationship

$$\langle F_x \rangle = 2c_e (\rho v_0^2 / 2) 2a = c_e \rho (v_0 / u_0)^2 u_0^2 2a,$$

where $\langle F_x \rangle$ and u_0 are defined by Eqs. (3.2), (4.3). Hence

$$c_e = 2\pi\delta^2 \frac{F_1}{(v_0/u_0)^2},$$

and with the parameter values used above ($\delta = 0.4$, $F_1 = 0.0100$, $v_0/u_0 = 0.23094$) $c_e = 0.188$; c_f^0 is defined by Eq. (5.1) and has the value 0.105.

Thus the resistance coefficient of the plate set in motion by the electromagnetic field is 1.8 times higher than the resistance coefficient of the classical plate.

Of the results obtained at $Re = 1180.60$ we will present the isolines $\Omega = \text{const}$ (Fig. 6, whereas in Figs. 2-5 the calculation region has been expanded in the y direction by a factor of four). It is evident that the latter are more elongated in the direction of the main flow and pressed closer to the plate (because of convective turbulence transfer) than the corresponding lines for $Re = 230.94$ (Fig. 4).

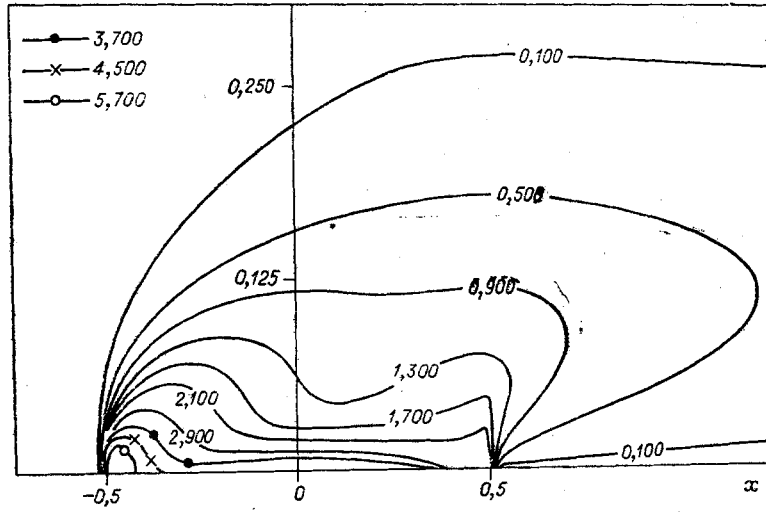


Fig. 4

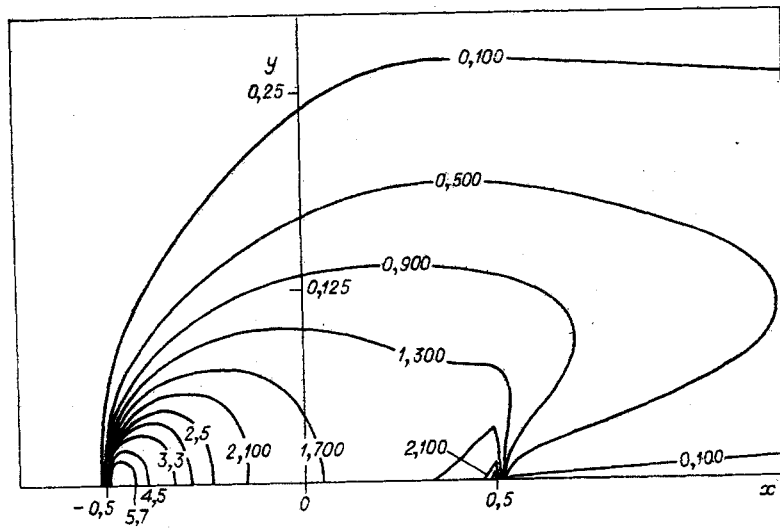


Fig. 5

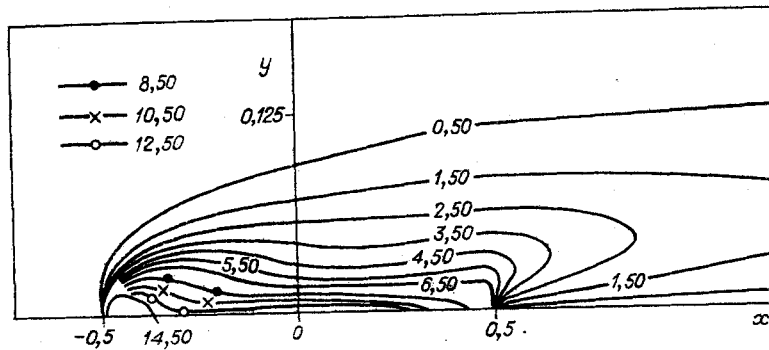


Fig. 6

In conclusion, we will present some of the dimensional quantities corresponding to plate motion with $Re^* = 3 \cdot 10^3$ in an electrolyte with $\sigma = 10^{12}$ 1/sec. Let $2a = 10^2$ cm. Then from Eq. (2.6) at $\delta = 0.4$ it follows that $\omega = 9 \cdot 10^4$ 1/sec, and from Eq. (4.4) and $v_0/u_0 = 0.39$ we have $v_0 = 1.2 \cdot 10^{-1}$ cm/sec; from Eq. (4.3), (2.5) we determine the amplitude of the maximum magnetic field intensity $H_0 = 2\pi I_0/\text{sec} \approx 2.7$ G.

LITERATURE CITED

1. I. M. Kirko, Liquid Metal in a Magnetic Field [in Russian], Énergiya, Moscow-Leningrad (1964).
2. O. M. Phillips, "Prospects for magnetohydrodynamic ship propulsion," J. Ship Res., 5, No. 4 (1962).
3. L. G. Vasil'ev and A. I. Khozhainov, Magnetohydrodynamics in Ship Technology [in Russian], Sudostroenie, Leningrad (1967).
4. V. I. Merkulov, "Motion of a sphere in a conductive liquid in the presence of crossed electric and magnetic fields," Magn. Gidrodin., No. 1 (1973).
5. A. Sneyd, "Generation of fluid motion in a circular cylinder by an unsteady applied magnetic field," J. Fluid Mech., 49, 4 (1971).
6. K. B. Dzhakupov, "Some difference schemes for the Navier-Stokes equations", Ch. M. M. S. S., 2, No. 1 (1971).
7. T. V. Kuskova, "Difference method for calculation of the flow of a viscous incompressible liquid," in: Calculation Methods and Programming [in Russian], 7th ed., Moscow State Univ. (1967).
8. V. I. Merkulov, V. I. Panchuk, and V. F. Tkachenko, "Solution of motion equations of an electrically conductive liquid in a longitudinal traveling magnetic field," in: Proceedings of the All-Union Seminar on Numerical Methods in Mechanics of a Viscous Liquid [in Russian], Nauka, Moscow (1969).
9. Tsan Sue-Sen, "The Poincaré-Lighthill-Ho Method," in: Problems in Mechanics [Russian translation], IL, Moscow (1959).
10. Z. Janour, "Resistance of a plate in a parallel flow at low Reynolds number," NACA TM No. 1316 (1951).

UNSTEADY FLOW OF A NON-NEWTONIAN LIQUID WITH A POWER RHEOLOGICAL LAW PAST A FLAT PENETRABLE PLATE

V. I. Vishnyakov and A. P. Shakhorin

UDC 532.526.2.53

We analyze the problem of the unsteady flow of a non-Newtonian liquid with a power rheological law past a flat penetrable plate. In contrast with [1], where a similarly posed problem is treated for a pseudoplastic liquid, we solve the problem for a dilatant liquid.

For a non-Newtonian liquid with a power rheological law, the relation between the shear stress τ and the velocity gradient $\partial u/\partial z$ for plane motion has the form [2]

$$\tau = k \left| \frac{\partial u}{\partial z} \right|^{n-1} \frac{\partial u}{\partial z} \quad (n > 0),$$

where k and n are rheological constants of the medium; the case $n = 1$ corresponds to Newtonian liquid, $n < 1$ to a pseudoplastic liquid, and $n > 1$ to a dilatant liquid.

The problem of the flow of a non-Newtonian liquid with a power rheological law past an infinite flat plate in the presence of uniform suction of liquid depending on time according to a definite law was treated in [1]. This problem was solved for pseudoplastic ($n < 1$) and Newtonian ($n = 1$) liquids. We solve the problem in a similar formulation without restriction on the possible values of $n > 0$.

Moscow. Translated from Zhurnal Prikladnoi Mekhaniki i Tekhnicheskoi Fiziki, No. 1, pp. 91-94, January-February, 1980. Original article submitted January 19, 1979.